

ESI for “Bayesian determination of the effect of a deep eutectic solvent on the structure of lipid monolayers”

Andrew R. McCluskey,^{ab‡} Adrian Sanchez-Fernandez,^{ac‡¶}
Karen J. Edler,^{a*} Stephen C. Parker,^a Andrew J. Jackson,^{cd}
Richard A. Campbell,^{ef} and Thomas Arnold^{abcg*}

^a Department of Chemistry, University of Bath, Claverton Down, Bath, BA2 7AY, UK.

^b Diamond Light Source, Harwell Campus, Didcot, OX11 0DE, UK.

^c European Spallation Source, SE-211 00 Lund, Sweden.

^d Department of Physical Chemistry, Lund University, SE-211 00 Lund, Sweden.

^e Institut Laue-Langevin, 71 avenue des Martyrs, 38000, Grenoble, France.

^f Division of Pharmacy and Optometry, University of Manchester, Manchester, M13 9PT, UK.

^g ISIS Neutron and Muon Source, Science and Technology Facilities Council, Rutherford Appleton Laboratory, Harwell Oxford, Didcot OX11 0QX, UK.

¶ Present address: Department of Food Technology, Lund University, SE-211 00 Lund, Sweden

1 Grazing incident X-ray diffraction (GIXD)

GIXD was measured for DPPC and DMPC at 30 mN m^{-1} at 22°C (and 7°C for DMPC), and are shown in Figures 1-3. All figures contain an artifact from the X-ray beam interacting with the Teflon of the Langmuir trough. However, in figures 1 and 3 it is possible to identify a (2, 0) diffraction peak that indicates the presence of a similar structure to that found under the same conditions in water.¹ Based on this information we believe that, similar to water, the phase of the lipid tails is likely to be in the liquid phase at all surface pressures measured.

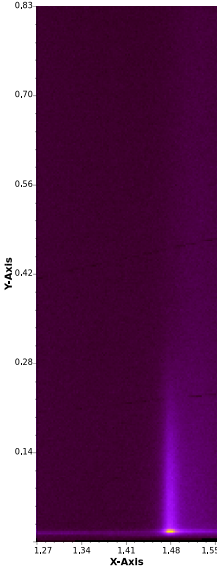


Figure 1: The GIXD pattern for DPPC at 30 mN m^{-1} at 22°C , the axes at in units of \AA^{-1} . Source: Datasets, figure files and running/plotting scripts are available under CC-BY.²

2 Probability distribution functions

The two-dimensional probability distribution functions (PDFs) for all parameters and all lipids from the X-ray reflectometry models are given in Figures 4-19. The two-dimensional probability distribution functions (PDFs) for all parameters and all lipids from the neutron reflectometry models are given in Figures 20-23.

References

- [1] E. B. Watkins, C. E. Miller, D. J. Mulder, T. L. Kuhl, and J. Majewski, *Phys. Rev. Lett.*, 2009, **102**, 238101.
- [2] A. McCluskey, *Figures for "Bayesian determination of the effect of a deep eutectic solvent on the structure of lipid monolayers"*, 2018, https://figshare.com/articles/_/6661784/0.

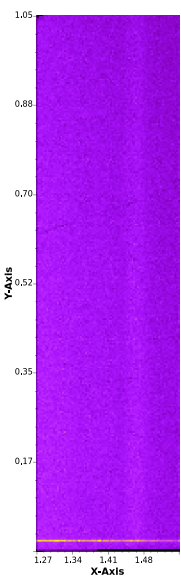


Figure 2: The GIXD pattern for DMPC at 30 mN m^{-1} at 22°C , the axes at in units of \AA^{-1} . Source: Datasets, figure files and running/plotting scripts are available under CC-BY.²

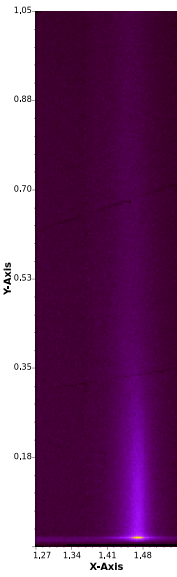


Figure 3: The GIXD pattern for DMPC at 30 mN m^{-1} at 7°C , the axes at in units of \AA^{-1} . Source: Datasets, figure files and running/plotting scripts are available under CC-BY.²

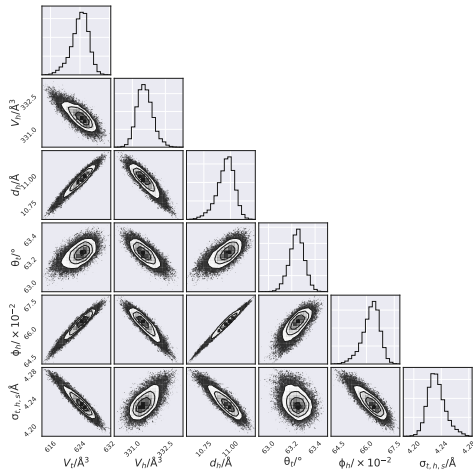


Figure 4: The multi-parameter PDFs for the chemically-relevant model of DLPC X-ray reflectometry data at 20 mNm^{-1} . Source: Datasets, figure files and running/plotting scripts are available under CC-BY.²

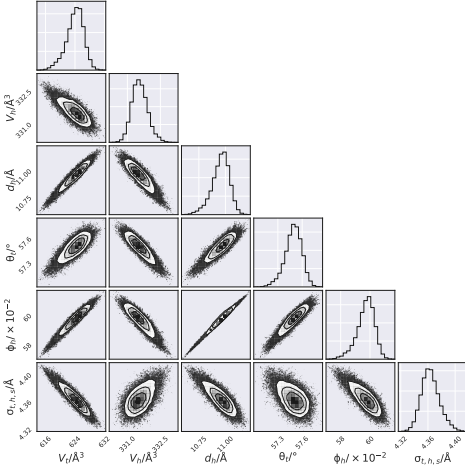


Figure 5: The multi-parameter PDFs for the chemically-relevant model of DLPC X-ray reflectometry data at 25 mNm^{-1} . Source: Datasets, figure files and running/plotting scripts are available under CC-BY.²

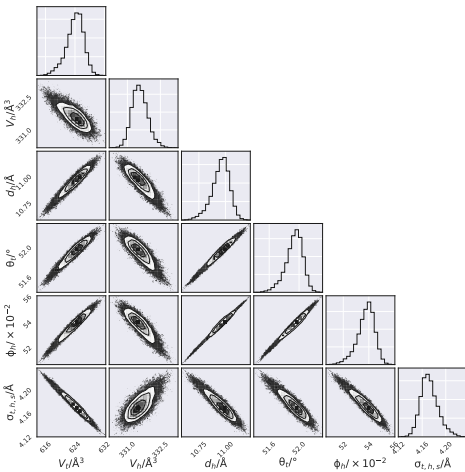


Figure 6: The multi-parameter PDFs for the chemically-relevant model of DLPC X-ray reflectometry data at 30 mNm^{-1} . Source: Datasets, figure files and running/plotting scripts are available under CC-BY.²

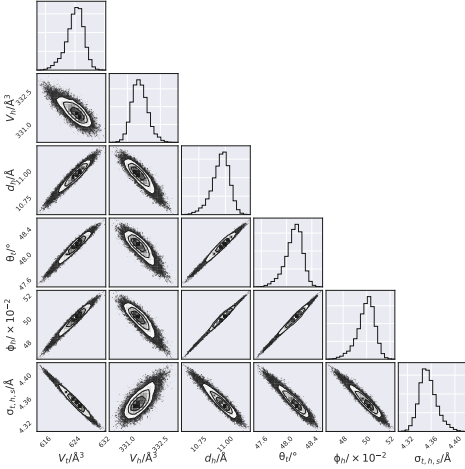


Figure 7: The multi-parameter PDFs for the chemically-relevant model of DLPC X-ray reflectometry data at 35 mNm^{-1} . Source: Datasets, figure files and running/plotting scripts are available under CC-BY.²

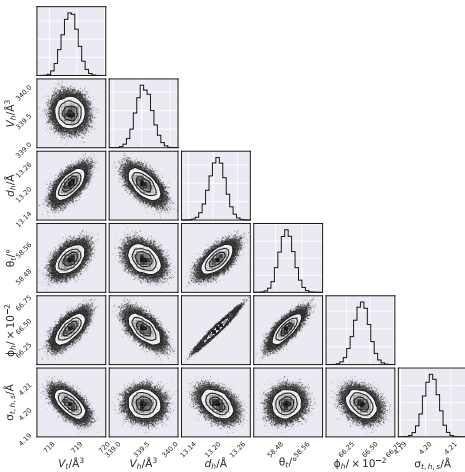


Figure 8: The multi-parameter PDFs for the chemically-relevant model of DMPC X-ray reflectometry data at 20 mNm^{-1} . Source: Datasets, figure files and running/plotting scripts are available under CC-BY.²

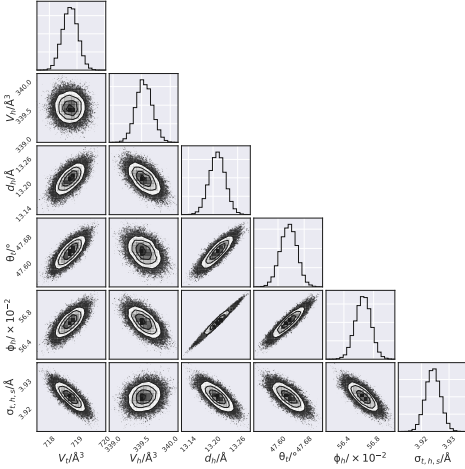


Figure 9: The multi-parameter PDFs for the chemically-relevant model of DMPC X-ray reflectometry data at 25 mNm^{-1} . Source: Datasets, figure files and running/plotting scripts are available under CC-BY.²

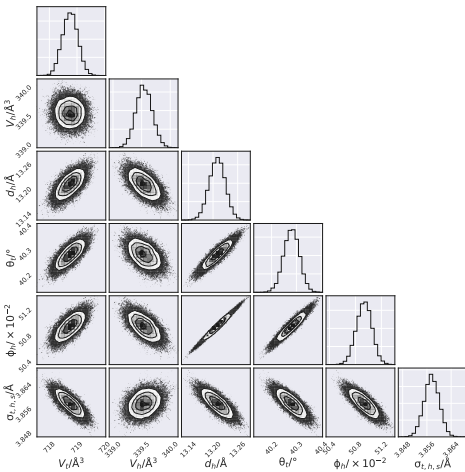


Figure 10: The multi-parameter PDFs for the chemically-relevant model of DMPC X-ray reflectometry data at 30 mNm^{-1} . Source: Datasets, figure files and running/plotting scripts are available under CC-BY.²

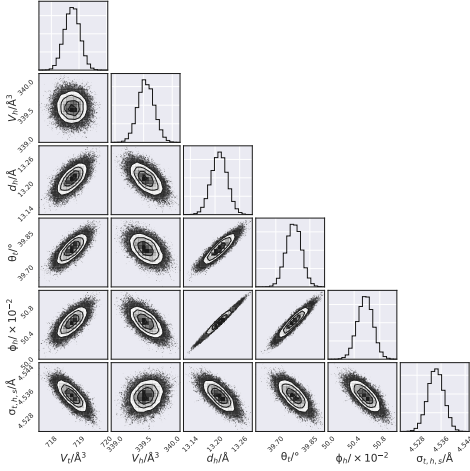


Figure 11: The multi-parameter PDFs for the chemically-relevant model of DMPC X-ray reflectometry data at 40 mNm^{-1} . Source: Datasets, figure files and running/plotting scripts are available under CC-BY.²

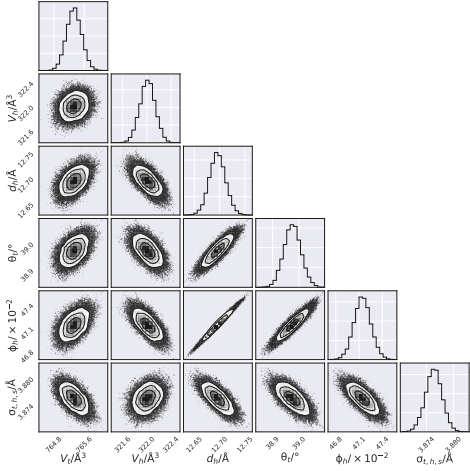


Figure 12: The multi-parameter PDFs for the chemically-relevant model of DPPC X-ray reflectometry data at 15 mNm^{-1} . Source: Datasets, figure files and running/plotting scripts are available under CC-BY.²

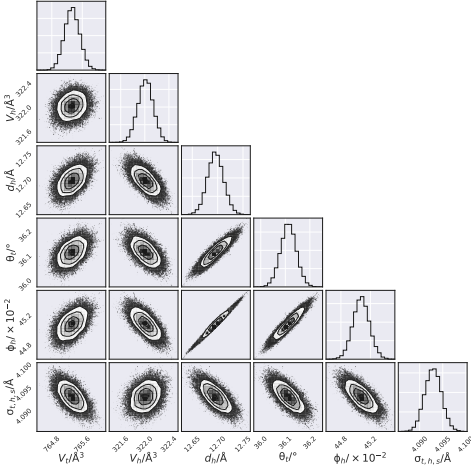


Figure 13: The multi-parameter PDFs for the chemically-relevant model of DPPC X-ray reflectometry data at 20 mNm^{-1} . Source: Datasets, figure files and running/plotting scripts are available under CC-BY.²

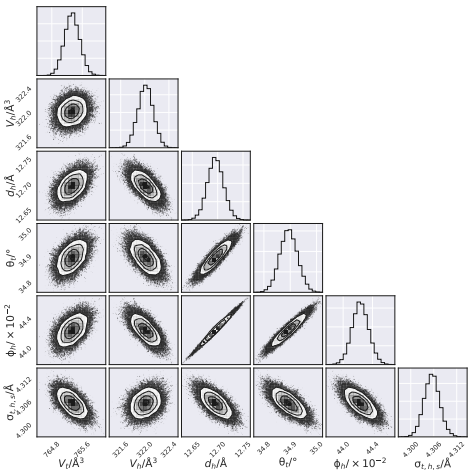


Figure 14: The multi-parameter PDFs for the chemically-relevant model of DPPC X-ray reflectometry data at 25 mNm^{-1} . Source: Datasets, figure files and running/plotting scripts are available under CC-BY.²

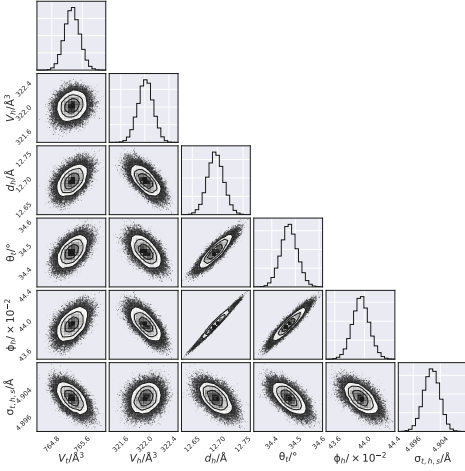


Figure 15: The multi-parameter PDFs for the chemically-relevant model of DPPC X-ray reflectometry data at 30 mNm^{-1} . Source: Datasets, figure files and running/plotting scripts are available under CC-BY.²

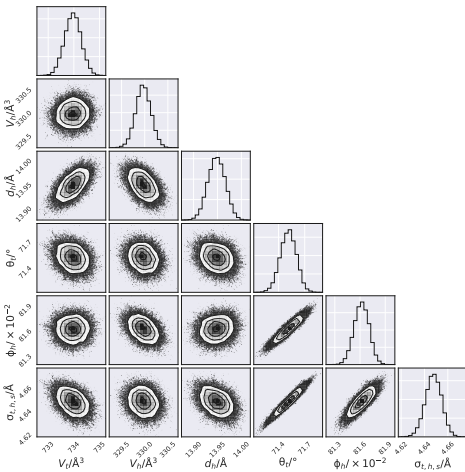


Figure 16: The multi-parameter PDFs for the chemically-relevant model of DMPG X-ray reflectometry data at 15 mNm^{-1} . Source: Datasets, figure files and running/plotting scripts are available under CC-BY.²

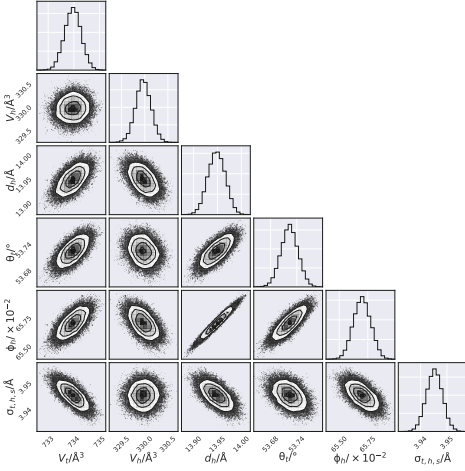


Figure 17: The multi-parameter PDFs for the chemically-relevant model of DMPG X-ray reflectometry data at 20 mNm^{-1} . Source: Datasets, figure files and running/plotting scripts are available under CC-BY.²

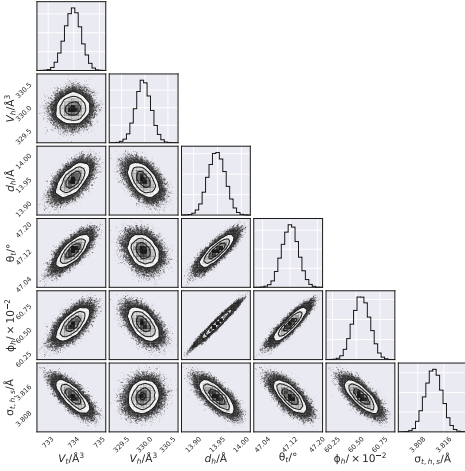


Figure 18: The multi-parameter PDFs for the chemically-relevant model of DMPG X-ray reflectometry data at 25 mNm^{-1} . Source: Datasets, figure files and running/plotting scripts are available under CC-BY.²

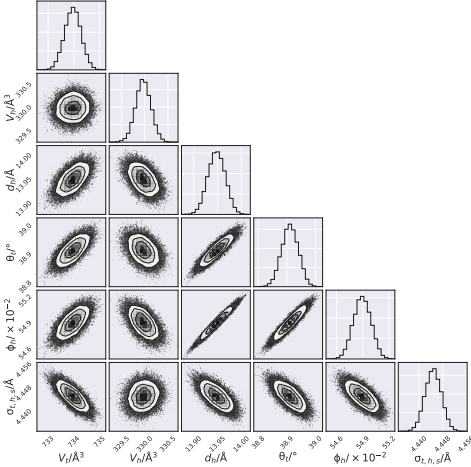


Figure 19: The multi-parameter PDFs for the chemically-relevant model of DMPG X-ray reflectometry data at 30 mNm^{-1} . Source: Datasets, figure files and running/plotting scripts are available under CC-BY.²

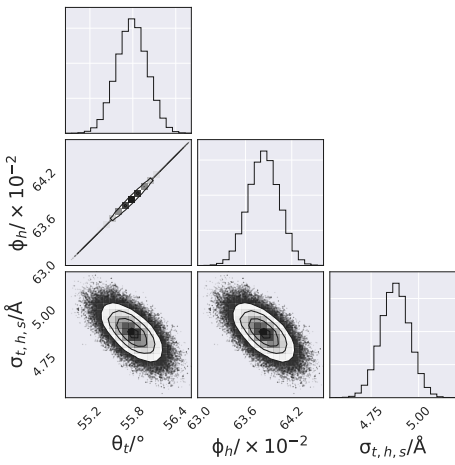


Figure 20: The multi-parameter PDFs for the chemically-relevant model of two contrast DMPC neutron reflectometry data at 20 mNm^{-1} . Source: Datasets, figure files and running/plotting scripts are available under CC-BY.²

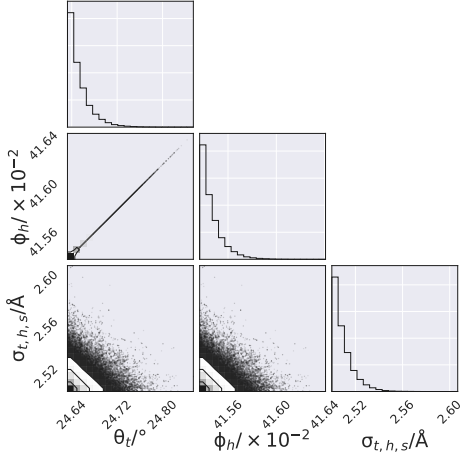


Figure 21: The multi-parameter PDFs for the chemically-relevant model of two contrast DMPC neutron reflectometry data at 25 mNm^{-1} . Source: Datasets, figure files and running/plotting scripts are available under CC-BY.²

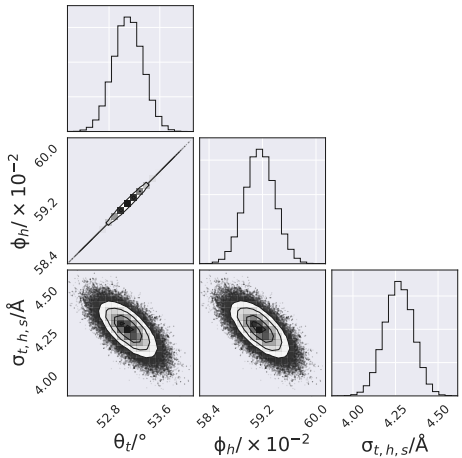


Figure 22: The multi-parameter PDFs for the chemically-relevant model of two contrast DPPC neutron reflectometry data at 15 mNm^{-1} . Source: Datasets, figure files and running/plotting scripts are available under CC-BY.²

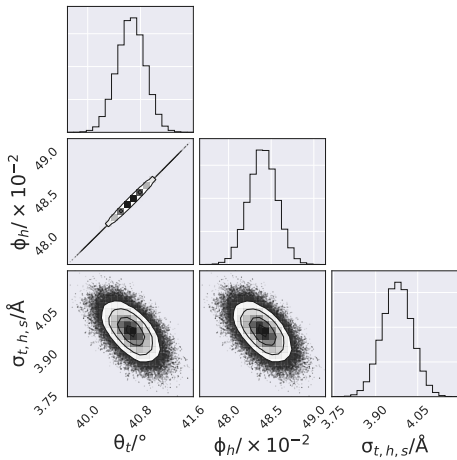


Figure 23: The multi-parameter PDFs for the chemically-relevant model of two contrast DMPC neutron reflectometry data at 20 mNm^{-1} . Source: Datasets, figure files and running/plotting scripts are available under CC-BY.²